actuators

MDPI

Article

Parameter Tuning Approach for Incremental Nonlinear Dynamic Inversion-Based Flight Controllers

Mark Henkenjohann [1,*], Udo Nolte [1], Fabian Sion [1], Christian Henke [1] and Ansgar Trächtler [2]

[1] Fraunhofer-Institute for Mechatronic Systems Design IEM, Zukunftsmeile 1, 33102 Paderborn, Germany; udo.nolte@iem.fraunhofer.de (U.N.); fabian.sion@iem.fraunhofer.de (F.S.); christian.henke@iem.fraunhofer.de (C.H.)

[2] Heinz Nixdorf Institute, Paderborn University, Fürstenallee 11, 33102 Paderborn, Germany; ansgar.traechtler@uni-paderborn.de

* Correspondence: mark.henkenjohann@iem.fraunhofer.de

Abstract: Incremental nonlinear dynamic inversion (INDI) is a widely used approach to controlling UAVs with highly nonlinear dynamics. One key element of INDI-based controllers is the control allocation realizing pseudo controls using available actuators. However, the tracking of commanded pseudo controls is not the only objective considered during control allocation. Since the approach only works locally due to linearization and the solution is often ambiguous, additional aspects like control efforts or penalizing the deviation of certain states must be considered. Conducting the control allocation by solving a quadratic program this results in a considerable number of weighting parameters, which must be tuned during control design. Currently, this is conducted manually and is therefore time consuming. An automated approach for tuning these parameters is therefore highly beneficial. Thus, this paper presents and evaluates a model-based approach automatically tuning the control allocation parameters of a tiltrotor VTOL using an optimization algorithm. This optimization algorithm searches for optimal parameters minimizing a cost functional that reflects the design target. This cost functional is calculated based on a test mission for the VTOL which is conducted within a simulation environment. The test mission represents the common operating range of the VTOL. The simulation environment consists of an aircraft model as well as a model of the INDI-based controller which is dependent on the control allocation parameters. On this basis, model-based optimization is conducted and the optimal parameters are identified. Finally, successful real-world tests on a 4-degrees-of-freedom testbench using the identified parameters are presented. Since the control allocation parameters can significantly influence the aircraft's stability, the 4-DOF testbench for the aircraft is required for rapid validation of the parameters at a minimum amount of risk.

Keywords: incremental nonlinear dynamic inversion; INDI; nonlinear control; Tiltrotor; VTOL; parameter tuning

Citation: Henkenjohann, M.; Nolte, U.; Sion, F.; Henke, C.; Trächtler, A. Parameter Tuning Approach for Incremental Nonlinear Dynamic Inversion-Based Flight Controllers. *Actuators* **2024**, *13*, 187. https://doi.org/10.3390/act13050187

Academic Editors: Andrea De Martin, Antonio Carlo Bertolino and Keigo Watanabe

Received: 29 March 2024
Revised: 6 May 2024
Accepted: 9 May 2024
Published: 13 May 2024

1. Introduction

Hybrid Vertical Take-Off and Landing Aircrafts (VTOLs) are a promising technology in the context of Advanced Air Mobility (AAM) applications. These aircraft configurations combine the advantages of multicopters and fixed-wing aircrafts. They are capable of conducting an energy-efficient airborne flight but do not require additional infrastructure like runways. A disadvantage of these aircrafts are their highly nonlinear dynamics. This results in a high complexity for stabilization and control. Therefore, advanced controller approaches like incremental nonlinear dynamic inversion (INDI) are utilized. This approach incrementally linearizes the nonlinear dynamics of an aircraft with respect to the so-called pseudo controls. INDI has already been adapted to various different aircraft configurations like multicopters [1–3] and planes [4,5] as well as hybrid aircrafts like tiltrotors [6–10], tiltwings [11–13], tailsitters [14], lift-and-cruise [15,16] and even more complex aircraft

configurations as presented in [17]. A key element of INDI is the control allocation, realizing the commanded pseudo controls by calculating setpoints for the actuators based on a simplified aircraft model. This can either be achieved by solving a quadratic programming problem as shown in [11,12,18], or by calculating a Moore–Penrose Inverse and conducting a null space transition as presented in [15,19]. Since hybrid VTOLs are usually over-actuated, i.e., the required forces and torque can be created by different actuators, the solution of control allocation is often ambiguous. Therefore, beside realization of pseudo controls, additional objectives can be included in the control allocation. This similarly applies to approaches solving the control allocation via quadratic programming [19] or via Moore–Penrose Inverse [11]. These additional objective functions typically penalize deviations of actuators from a certain value and high-frequency oscillations of actuators. Due to the large number of actuators this results in a large number of weighting parameters which must be tuned during control design. Hence, the parameter tuning can be very time consuming when conducted manually. Thus, automated parameter identification for the control allocation would be highly beneficial in terms of tuning efforts.

Currently, no research has been conducted regarding automated tuning of the control allocation parameters of an INDI-based controller. Thus, this paper presents and evaluates an automated parameter tuning approach for the control allocation of an INDI-based controller. The parameters are identified using an optimization algorithm which minimizes a cost functional. This cost functional reflects the design target and is calculated based on a representative test mission performed by an aircraft in a simulation environment. The simulation environment contains a model of the aircraft which is controlled by the INDI-based controller. The behavior of the INDI-based controller is dependent on the control allocation parameters. These can be defined by the optimization algorithm during the parameter tuning process.

Therefore, the remainder of the paper is structured as follows: In Section 2, the fundamentals of incremental nonlinear dynamic inversion are presented. Section 3 presents the tiltrotor VTOL aircraft configuration for validation of the automatically identified parameter sets. The INDI-based controller approach for the aircraft under consideration is presented in Section 4. In Section 5, the automated parameter tuning approach is presented. Section 6 presents and evaluates model-based results first. Afterwards a 4-degrees-of-freedom testbench is presented. Using this 4-DOF testbench, risk-minimized real-world validation of the automated parameter tuning is conducted. Section 7 consists of a conclusion and future work.

2. Incremental Nonlinear Dynamic Inversion

The following section outlines the fundamentals of incremental nonlinear dynamic inversion (INDI) based on, e.g., [6,19,20]. INDI is an incremental formulation of nonlinear dynamic inversion (NDI) which is also known as input–output linearization from general control theory. This approach linearizes the dynamics of highly nonlinear systems by inverting a dynamic model of the system [21]. In contrast to that, INDI conducts the inversion of the system using a linear Taylor series approximation of the system dynamics in each timestep. The system under consideration is a nonlinear, non-affine multiple-input–multiple-output system

$$\begin{aligned} \dot{\underline{x}} &= \underline{f}(\underline{x}, \underline{u}) \\ \underline{y} &= \underline{h}(\underline{x}, \underline{u}), \end{aligned} \tag{1}$$

with the state variable $\underline{x} \in \mathbb{R}^n$, the input variable $\underline{u} \in \mathbb{R}^p$, and the output variable $\underline{y} \in \mathbb{R}^q$. The vector fields $\underline{f} : \mathcal{D}_{\underline{x},\underline{u}} \to \mathbb{R}^n$, $\underline{h} : \mathcal{D}_{\underline{x},\underline{u}} \to \mathbb{R}^q$ are sufficiently smooth and differentiable. For the purpose of linearization, we determine the relative degree r_i which is the order of the first time derivative of the output variable y_i explicitly dependent on the input $\underline{u}$. Generally, $y_i^{(r_i)}$ equals a nonlinear function dependent on $\underline{x}$ and $\underline{u}$ which is denoted with $F_i(\underline{x}, \underline{u})$ for $i = 1, \ldots, q$. The overall relative degree of the system is defined as

$$r = \sum_{i=1}^{q} r_i. \tag{2}$$

On this basis, the so-called pseudo control variables $\underline{\nu}$ serving as new input variables can be defined with

$$\underline{\nu} = \begin{bmatrix} \nu_1 \\ \vdots \\ \nu_q \end{bmatrix} := \begin{bmatrix} y_1^{(r_1)} \\ \vdots \\ y_q^{(r_q)} \end{bmatrix} = \begin{bmatrix} F_1(\underline{x}, \underline{u}) \\ \vdots \\ F_q(\underline{x}, \underline{u}) \end{bmatrix} = \underline{F}(\underline{x}, \underline{u}). \tag{3}$$

Hence, the r_i-th derivative of $\underline{y_i}$ can be assigned arbitrarily using the pseudo control input ν_i. Additionally, new states $\underline{\zeta_i}$ are introduced as follows:

$$\underline{\zeta_i} = \begin{bmatrix} \zeta_{i,1} \\ \vdots \\ \zeta_{i,r_i} \end{bmatrix} = \begin{bmatrix} y_i^{(0)} \\ \vdots \\ y_i^{(r_i-1)} \end{bmatrix}, \; i = 1, \ldots, q. \tag{4}$$

The new overall state vector can be denoted with

$$\underline{\zeta} = \begin{bmatrix} \underline{\zeta_1} \\ \vdots \\ \underline{\zeta_q} \end{bmatrix}. \tag{5}$$

Using the new states and pseudo control variables the linearized system representation can be derived as shown, for example, in [6]. To realize that $y_i^{(r_i)}$ follows the desired pseudo control input $\nu_{i,des}$ for $i = 1, \ldots, q$ the required input vector $\underline{u}$ must be determined. Thus, the equation

$$\underline{\nu}_{des} = \underline{F}(\underline{x}, \underline{u}). \tag{6}$$

must be solved for $\underline{u}$. In the case of INDI this is achieved by linearizing $\underline{F}$ in the current state as follows:

$$\underline{F}(\underline{x}, \underline{u}) \approx \underbrace{\underline{F}(\underline{x}_0, \underline{u}_0)}_{\underline{\nu}_0} + \underbrace{\left.\frac{\partial F}{\partial \underline{x}}\right|_{\underline{x}_0, \underline{u}_0}}_{\underline{A}_0(\underline{x}_0, \underline{u}_0)} \cdot \Delta \underline{x} + \underbrace{\left.\frac{\partial F}{\partial \underline{u}}\right|_{\underline{x}_0, \underline{u}_0}}_{\underline{B}_0(\underline{x}_0, \underline{u}_0)} \cdot \Delta \underline{u}, \tag{7}$$

where $\underline{x}_0, \underline{u}_0, \underline{\nu}_0$ are the current state, input variable, and pseudo control variable. $\underline{B}_0$ is called the control effectiveness matrix. Since the actuator dynamics are much faster than the aircraft dynamics, the term $\underline{A}_0 \cdot \Delta \underline{x}$ can be omitted. This assumption is called the time scale separation principle and simplifies Equation (7) to

$$\underline{F}(\underline{x}, \underline{u}) \approx \underline{\nu}_0 + \underline{B}_0(\underline{x}_0, \underline{u}_0) \cdot \Delta \underline{u}. \tag{8}$$

This can be inserted into Equation (6) and solved for $\Delta \underline{u}$ using the uniquely defined Moore–Penrose Inverse

$$\Delta \underline{u} = \underline{B}_0^+(\underline{x}_0, \underline{u}_0) \cdot \underbrace{(\underline{\nu}_{des} - \underline{\nu}_0)}_{\Delta \underline{\nu}} \tag{9}$$

Thus, the required control input $\underline{u}$ realizing the desired pseudo control input $\underline{\nu}_{des}$ can be calculated by

$$\underline{u} = \underline{u}_0 + \underline{B}_0^+(\underline{x}_0, \underline{u}_0) \cdot \Delta \underline{\nu}. \tag{10}$$

However, for the remainder of this paper we choose another possibility, calculating $\Delta \underline{u}$ equivalent to Equation (9) solving the following quadratic program:

$$\Delta \underline{u} = \arg\min_{\Delta \underline{u}} (\underline{B}_0 \cdot \Delta \underline{u} - \Delta \underline{\nu})^T \cdot (\underline{B}_0 \cdot \Delta \underline{u} - \Delta \underline{\nu}) \tag{11}$$

choosing the input variable increment $\Delta \underline{u}$ such that the quadratic error between the desired pseudo control increment $\Delta \underline{\nu}$ and the realized pseudo control increment according to $\underline{B}_0 \cdot \Delta \underline{u}$ is minimized. In the case of Tiltrotor VTOLs, $q < p$ usually applies; i.e., the number of pseudo controls is smaller than the input variables. Thus, the solution of the optimization problem in (11) is ambiguous. Hence, the cost functional of Equation (11) can be generalized by adding additional penalty functions and constraints. The generalized optimization problem can be written as follows:

$$\begin{aligned} \Delta \underline{u} = \quad & \arg\min_{\Delta \underline{u}} (\underline{B}_0 \cdot \Delta \underline{u} - \Delta \underline{\nu})^T \cdot \underline{W}\left(\underline{p}\right) \cdot (\underline{B}_0 \cdot \Delta \underline{u} - \Delta \underline{\nu}) + J_{\underline{u}}\left(\underline{p}\right) + J_{\Delta \underline{u}}\left(\underline{p}\right) \\ \text{s.t. } & \max(\Delta \underline{u}_{min}, \underline{u}_{min} - \underline{u}_0) \leq \Delta \underline{u} \leq \min(\Delta \underline{u}_{max}, \underline{u}_{max} - \underline{u}_0). \end{aligned} \tag{12}$$

$\underline{W}$ is a diagonal matrix prioritizing pseudo controls. $J_{\underline{u}}$ is a cost functional penalizing deviations of predefined values preventing, for example, actuator fighting. $J_{\Delta \underline{u}}$ is a cost functional penalizing large increments $\Delta \underline{u}$ avoiding high-frequency oscillations. These additional cost functionals contain additional weighting parameters $\underline{p}$ which must be tuned during control design.

3. Aircraft Description

This section presents the considered aircraft configuration for validation of the automated parameter tuning approach presented in Section 5. The aircraft is a tiltrotor VTOL with highly nonlinear dynamics and is therefore a typical application scenario for an INDI-based controller. Thus, this aircraft is well suited for validation of the automated parameter tuning approach presented in this paper.

The relevant coordinate frames describing the aircraft are shown in Figure 1. Assuming a flat earth, the geodetic coordinate frame g is defined as a North-East-Down (NED) frame. The ${}_f x$-axis of the body-fixed frame f points towards the nose of the aircraft, the ${}_f y$-axis points to the right side and the ${}_f z$-axis points downwards from the aircraft's perspective. The horizontal frame h is the control frame where the ${}_h x$-axis is the projection of the body-fixed ${}_f x$-axis into the ${}_g \mathrm{x} - {}_g \mathrm{y}$-plane and the ${}_h z$-axis is identical to the geodetic ${}_g z$-axis.

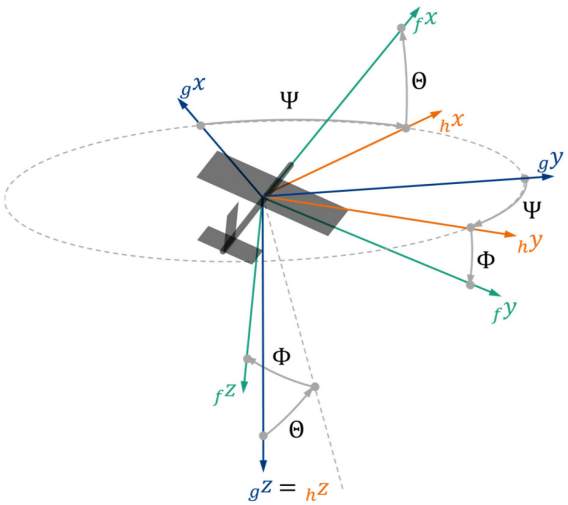

Figure 1. Relevant coordinate frames of the tiltrotor VTOL.

The tiltrotor VTOL configuration is schematically shown in Figure 2. It consists of four propellers attached to four tilting mechanisms, respectively. In addition, the aircraft is equipped with a main wing as well as a tail. In terms of control surfaces, two ailerons are attached to the main wing and the tail consists of an elevator and a rudder. The propeller rotational speeds are defined as $\omega_{Pi}, i = 1, \ldots, 4$ and the tilt angles are defined

as $\delta_i, i = 1, \ldots, 4$. Additionally, the aileron deflections are described as ξ_1, ξ_2, the elevator deflection as η_1, and the rudder deflection as η_2. Using the propellers, the aircraft can take-off and land vertically. By tilting the propellers, a transition from multicopter to airborne mode and vice versa is possible. Since the aircraft consists of twelve actuators and only six degrees of freedom must be stabilized, it is an over-actuated aircraft. In other words, it is ambiguous which actuators are used in order to create a certain force or torque. Thus, using an INDI approach additional cost functionals must be considered during control allocation in order to achieve reasonable dynamic behavior. Therefore, this tiltrotor VTOL configuration is a suitable test system for validating the automated parameter tuning approach.

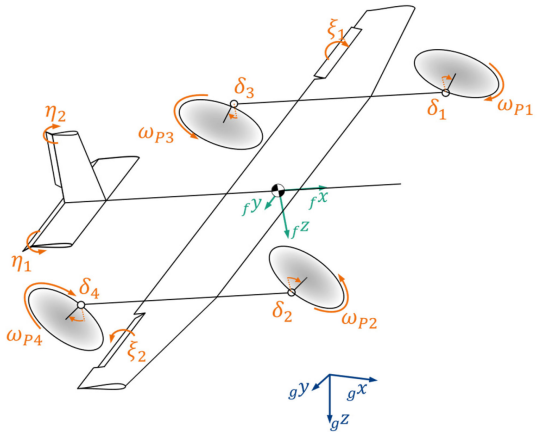

Figure 2. Tiltrotor VTOL configuration.

4. Controller Approach

This paper presents and investigates an automated parameter tuning approach for the control allocation of an INDI-based controller for a tiltrotor VTOL. Therefore, the underlying controller approach must be outlined first. The approach is based on [22]. The controller structure is illustrated in Figure 3 and can be subdivided into the main functionalities of velocity control, attitude control as well as sensor data fusion/observers. It is a cascaded INDI approach, separately linearizing rotational and translational dynamics since the rotational dynamics are required to influence the translational dynamics. The approach utilizes propellers and tilt angles creating rotational and translational dynamics at the same time. Typically, the output variables of VTOLs consist of the translational velocities in horizontal frame, as well as the roll angle, pitch angle, and the yaw rate, thus $\underline{y} = \begin{bmatrix} {}_hu_k & {}_hv_k & {}_hw_k & \Phi & \Theta & \dot{\Psi} \end{bmatrix}^T$. Since rotational dynamics and translational dynamics are linearized separately, the output variables must be split as well into outer output variables and inner output variables.

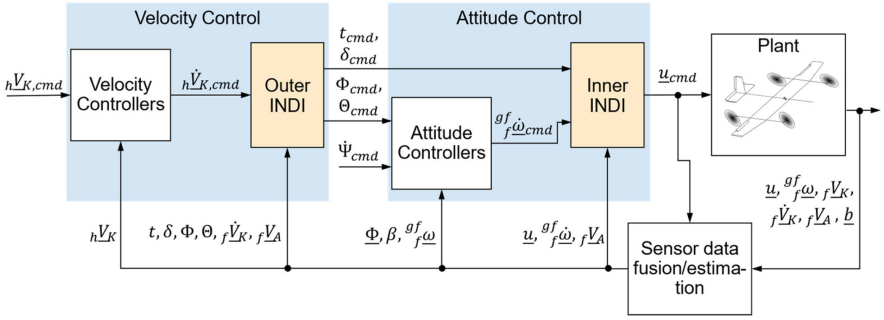

Figure 3. Cascaded INDI-based controller structure for the Tiltrotor VTOL.

4.1. Velocity Control

The outer output variables obviously consist of translational velocities $\underline{y}_O = \begin{bmatrix} {}_h u_k & {}_h v_k & {}_h w_k \end{bmatrix}^T$. Thus, the outer pseudo control variables $\underline{\nu}_O$ consist of translational accelerations ${}_h\dot{\underline{V}}_k$ because these are directly influenced by the forces acting on the aircraft. Since actuator dynamics are neglected in INDI, these forces are directly dependent on the input variables. Hence, as depicted in Figure 3, the outer loop of the presented controller approach consists of velocity controllers calculating commands for the outer pseudo controls. These are typical PID controllers. The commanded pseudo controls are then realized by the outer INDI. For that purpose, the outer INDI calculates setpoints for the outer loop input variables $\underline{u}_O = \begin{bmatrix} \Phi_{cmd} & \Theta_{cmd} & t_{cmd} & \delta_{cmd} \end{bmatrix}^T$. As already stated, rotational dynamics are required to control lateral and vertical translational dynamics. Creating a lateral acceleration is, for example, only possible using the roll angle. Creating a vertical acceleration in airborne mode is achieved using the pitch angle. Thus, roll angle and pitch angle are considered as so-called virtual input variables since these are not input variables in the original sense, but they are suitable for creating translational accelerations. Additionally, t_{cmd} and δ_{cmd} are also virtual input variables and describe the overall specific thrust and the overall tilt angle, respectively. The specific thrust can be calculated as

$$t = \frac{\left\| \sum_i \underline{F}_{P,i} \right\|_2}{m}, \tag{13}$$

and is therefore describing the overall amount of thrust related to the mass created by the propellers of the Tiltrotor VTOL. The overall tilt angle can be calculated by

$$\delta := \arctan \frac{F_{P,x}}{-F_{P,z}}, \tag{14}$$

and is therefore describing the direction of the thrust created by the propellers in relation to the body-fixed frame of the aircraft. Summing up, t and δ describe all the relevant characteristics of the propellers and tilt angles for creating translational accelerations. By introducing these virtual input variables, it is possible to realize a cascaded controller structure and at the same time utilize the propellers and tilt angles, creating rotational and translational accelerations.

The translational accelerations are realized solving the optimization problem shown in Equation (12). In order to gain reasonable dynamic behavior, the penalty terms are structured as follows:

$$J_{\underline{u}}\left(\underline{p}\right) = \sum_i p_{u_i} \cdot J_{u_i} \tag{15}$$

where p_{u_i} are the weighting factors and J_{u_i} are the penalty terms penalizing deviations of the actuator deflections from a predefined value $u_{i,ref}$ as follows:

$$J_{u_i} = \left(u_{i,0} + \Delta u_i - u_{i,ref} \right)^2. \tag{16}$$

In terms of the outer INDI, the deviation of the overall tilt angle from the forward position must be penalized in case the aerodynamic speed is faster than the stall speed. This ensures an energy-efficient airborne flight. Thus, the weighting factor p_δ is dependent on the aerodynamic velocity. In addition, the deviation of the pitch angle Θ from zero is penalized, ensuring that the pitch angle and tilt angle, which are redundant in hover mode, do not compensate for each other. This also prioritizes using the tilt angle for forward acceleration over using the pitch angle which is reasonable from an energy point of view.

In addition to that, the incremental deflection of the input variables is penalized using

$$J_{\Delta\underline{u}}\left(\underline{p}\right) = \sum_i p_{\Delta u_i} \cdot \Delta u_i^2 \tag{17}$$

thus avoiding high-frequency oscillations. In the outer loop, this is used with a fixed weight for all virtual input variables.

4.2. Attitude Control

The virtual input variables commanded from the velocity control loop are realized by the attitude control which is the inner cascade. Thus, the output variables of the inner loop are $\underline{y}_I = \begin{bmatrix} \Phi & \Theta & \dot{\Psi} & t & \delta \end{bmatrix}^T$. Consequently, rotational accelerations ${}^{gf}_{f}\underline{\omega}$ belong to the pseudo controls of the inner loop since these are directly influenced by the torque which is directly dependent on the input variables neglecting the actuator dynamics. In addition, t and δ belong to the pseudo control variables because they are directly dependent on the input variables. Thus, t_{cmd} and δ_{cmd} are directly fed into the control allocation. The attitude setpoints are forwarded into attitude controllers. These are typical PID controllers, calculating setpoints for the rotational accelerations. The rotational accelerations, as well as specific thrust and overall tilt angle, are realized by the inner INDI calculating necessary input variables. By realizing the specific thrust and overall tilt angle the inner INDI creates the required thrust in the required direction to generate the commanded translational accelerations of the outer INDI. At the same time, the inner INDI can use propellers and tilt angles to generate rotational accelerations. In this way, a cascaded INDI structure is realized, which can use propellers and tilt angles to realize rotational and translational accelerations.

The inner loop control allocation is structured like the outer loop control allocation, consisting of penalty terms for absolute as well as incremental actuator deflections. The penalty term for absolute actuators deflections is structured as shown in Equations (15) and (16). In terms of the propellers a deviation of the average propeller rotational speed is penalized in order to ensure that all propellers are used. Otherwise, this would not automatically be the case, since it is possible to stabilize the aircraft using three propellers and the tilt angles as well. Additionally, the deviation of the tilt angles δ_i from the commanded overall tilt angle δ_{cmd} is penalized. This ensures that that the single tilt angles only deviate from the commanded overall tilt angle in case they are required for creating another rotational acceleration. In terms of the flaps, the deviation from their neutral position is penalized to avoid, for example, the ailerons compensating for each other.

4.3. Sensor Data Fusion/Estimation

In addition to velocity and attitude control, sensor data fusion/estimation are an important part of the controller structure. The structure of the implemented sensor data fusion/estimation is shown in Figure 4. The aircraft is equipped with the following sensors: an inertial measurement unit, for measuring translational acceleration ${}_{f}\dot{\underline{V}}_K$ as well as rotational speed ${}^{gf}_{f}\underline{\omega}$; a magnetometer, for measuring the earth's magnetic field $\underline{b}$; a GNSS sensor, for measuring the position ${}_{g}\underline{s}$; as well as a pitot tube, for measuring aerodynamic speed ${}_{f}u_A$ in the body-fixed ${}_{f}x$-direction. Based on these measurements, an Extended Kalman Filter (EKF) which is pre-implemented on the development platform, estimates the attitude $\underline{\Phi}$, the velocity ${}_{f}\underline{V}_K$, and the aerodynamic speed ${}_{f}\underline{V}_A$. Estimation of actuator states as well as rotational accelerations is especially interesting since these are variables which are often not measured or estimated by the development platform and are specifically required for INDI. The estimation of actuator states is conducted using rate-limited PT1-models as an actuator model. The necessary parameters have been identified experimentally. Since the actuators are all stationary accurate regarding their setpoints, this approach works under normal conditions. If measurements are available, these can be used to increase the estimation accuracy using an observer. In addition to that, all measurements are filtered using a PT2 filter. It is important to filter all estimations and measurements with that filter to make sure all variables have the same phase delay. This is critical in order to ensure stability as shown in [23]. Since the translational acceleration and speed are measured in a body-fixed frame they are transformed to the horizontal frame. The required rotational acceleration ${}^{gf}_{f}\dot{\underline{\omega}}$ can be determined by calculating the derivative

of the filtered ${}_{f}^{gf}\underline{\omega}_{f}$. However, although the variable is already filtered, the remaining noise influences the aircraft dynamics. Decreasing the cutoff frequency, on the other hand, results in a phase delay which also significantly influences the aircraft dynamics. Thus, a complementary filter, as shown for example in [24], is used in order to determine the angular acceleration with minimum noise and also no phase delay with regard to the already filtered variables. The complementary filter uses, on the one hand, an additional lowpass filter, and then derives the filtered angular velocity. On the other hand, the angular acceleration is determined based on an aircraft model. Afterwards, this model-based angular acceleration is high-pass filtered. This way, the fast dynamics are determined by the model and the slow dynamics are determined using the measurements.

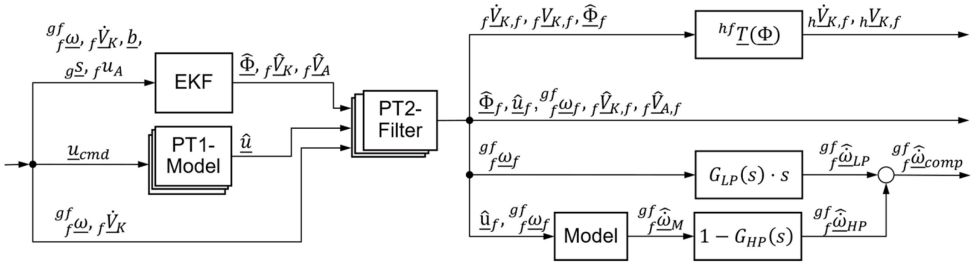

Figure 4. Sensor data fusion/estimator structure.

5. Automatic Parameter Tuning Approach

In this section, the automated parameter tuning approach is presented. Since the computing time of optimization problems increases exponentially with their dimensions, the identification of the inner and outer control allocation parameters is conducted separately. The aim of this paper is to validate whether and how automated parameter tuning of control allocation parameters is possible. Thus, for the sake of simplicity, this paper focuses on the parameter tuning approach for the attitude control loop. The structure of the approach is shown in Figure 5. The approach consists of test missions, a simulation environment, an objective function G, as well as an optimization algorithm. The test missions consist of reference trajectories for the output variables of the attitude control loop. These test missions must represent the typical operating range of the aircraft. The simulation environment consists of a physical model of the aircraft as well as the whole controller structure. Within that simulation environment, the dynamic behavior of the controlled aircraft is simulated while flying the test mission. Based on that simulation, an objective function is calculated quantifying the controller quality. The objective function values are forwarded to an optimization algorithm. Based on that, it implements different parameter configurations $\underline{p}$ into the controller. In the following subsections, these different elements of the automated parameter tuning approach are presented in more detail.

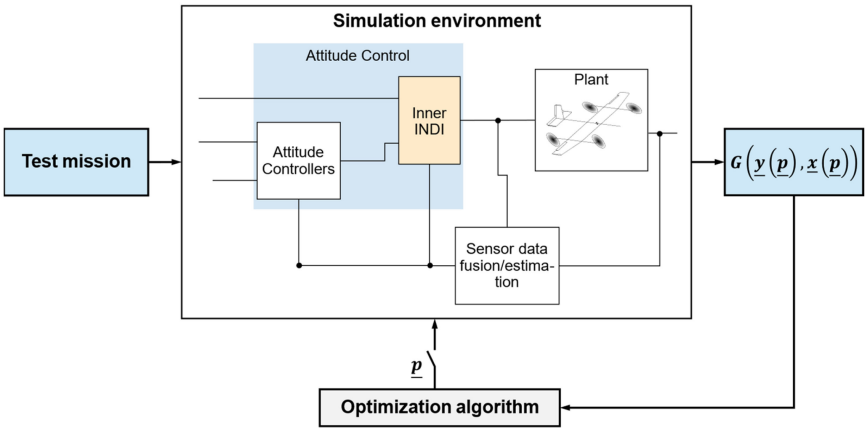

Figure 5. Structure of the automated parameter tuning approach.

5.1. Simulation Environment

The simulation environment consists of a model of the presented controller structure as well as a physical model of the aircraft. Since the controller approach has already been presented in Section 3, this section focuses on the elaboration of the physical aircraft model. A block diagram of the model is shown in Figure 6. The basic structure of the model is based on [25,26] and was adapted to a tiltrotor VTOL. The model consists of actuator models, a propeller model, an aerodynamic model, a gravity model, equations of motion, as well as a sensor model. The inputs into the model are the commands for the actuator states.

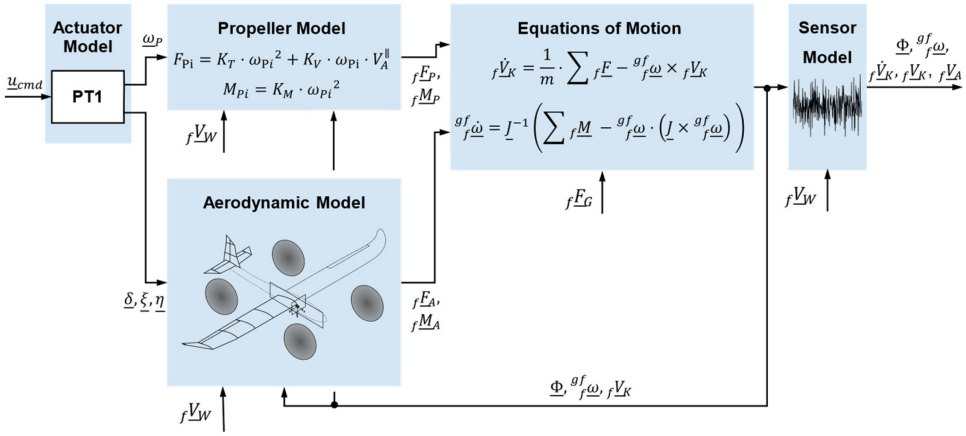

Figure 6. Structure of the aircraft model.

The actuator dynamics are modeled using rate limited PT1-models. It is important to model the actuator dynamics in order to validate whether the time scale separation principle is valid for that specific aircraft. Based on the current propeller rotational speeds and the aerodynamic state, the propeller thrust and torque are calculated using a simplified propeller model from [11]. The propeller force and torque can be calculated by

$$\begin{aligned} F_{Pi} &= K_T \cdot \omega_{Pi}{}^2 + K_V \cdot \omega_{Pi} \cdot V_A^{\parallel} \\ M_{Pi} &= K_M \cdot \omega_{Pi}{}^2,\ i = 1,\ldots,4, \end{aligned} \tag{18}$$

where K_T, K_V, K_M are propeller constants and $V_A^{\parallel}$ is the aerodynamic velocity perpendicular to the propeller disc. Based on the aircraft geometry, the propeller forces and torque are then summarized into a resulting propeller force ${}_f\underline{F}_P$ and torque ${}_f\underline{M}_P$.

The aerodynamic forces and torque are calculated using a component-based aerodynamic model as presented in, e.g., [26,27]. Therefore, the wing and tail of the aircraft are subdivided into aerodynamic elements having a triangular, rectangular, or trapezoidal shape as shown in Figure 6. The local aerodynamic conditions are calculated for each element. Based on the aerodynamic conditions, the control surface deflections as well as the aerodynamic coefficients of the airfoil obtained from a combination of potential flow simulations and an extrapolation the forces and torque of each aerodynamic element are calculated. These forces and torque are then summarized into a resulting aerodynamic force ${}_f\underline{F}_A$ and torque ${}_f\underline{M}_A$. Important aspects modeled here are the aerodynamic damping effects, which according to [11], are important to consider during design of an INDI-based controller. Interactions between the aerodynamic structures and the propeller downwash are neglected since the INDI approach is very robust against model uncertainties.

Gravity is also considered within the model. It is modeled as a constant external force ${}_f\underline{F}_G$ applied at the aircraft's center of gravity.

The calculated propeller and aerodynamic forces and torque, as well as the gravitational force, are included in the equations of motion. The aircraft is considered as a rigid body neglecting the elasticity of the aircraft and the gyroscopic effects of the propellers.

Additionally, the moments of inertia are assumed to be constant. Tilting the propellers results in a maximum change in the inertia of approximately 7.5%. Since the rotational equations of motion are linearly dependent on the inertia, the modeling error committed by this assumption is smaller than 7.5%. Due to the robustness of INDI against modeling uncertainties, as shown in [11], the change in the inertia resulting from tilting propellers is neglected. Hence, the equations of motion are as follows:

$$\begin{aligned} {}_f\dot{\underline{V}}_K &= \tfrac{1}{m}\cdot\left({}_f\underline{F}_A + {}_f\underline{F}_P + {}_f\underline{F}_G\right) - {}^{gf}_{f}\underline{\omega} \times {}_f\underline{V}_K \\ {}^{gf}_{f}\dot{\underline{\omega}} &= \underline{J}^{-1}\left({}_f\underline{M}_A + {}_f\underline{M}_P - {}^{gf}_{f}\underline{\omega}\cdot\left(\underline{J}\times {}^{gf}_{f}\underline{\omega}\right)\right) \end{aligned} \tag{19}$$

The rotational and translational states are calculated by numeric integration of the equations of motion as well as required coordinate transformations.

The last part of the model is a sensor model. This is particularly important since the measurements of angular velocities are typically very noisy. Thus, the sensor noise can have a negative impact on the aircraft dynamics which is also tackled using the incremental penalty functions shown in Equation (17). The sensor noise is modeled using white noise.

5.2. Objective Function

The aim of the presented approach is to find a set of parameters $\underline{p}$ for the control allocation so that the controller quality is maximized. Formally, this can be written as a minimization problem:

$$\underline{p} = \text{argmin} G\left(\underline{p}\right) \tag{20}$$

This means that the weighting parameters are the optimization variables. The objective function G describes the design target quantitatively as a function of the weighting parameters $\underline{p}$. The aim of the optimization is to set the weights of the control allocation in such a way that a high control quality is achieved in the normal operating range of the aircraft. Therefore, the following cost functional is proposed:

$$\mathrm{G}\left(\underline{p}\right) = g_y\left(\underline{y}\left(\underline{p}\right)\right) + \gamma\cdot g_x\left(\underline{x}\left(\underline{p}\right)\right) \tag{21}$$

Within that cost functional, g_y is a term quantifying the tracking error of the output variables $\underline{y}$ which is obviously the main target of the controller. Additionally, g_x is an additional state-dependent cost functional where additional optimization objectives can be considered, which are not observable through the output variables. This additional cost functional is weighted by the weighting factor γ. It is important to ensure that no other weighting factors are included within the cost functionals, since otherwise the parameter tuning approach would not reduce efforts; this would then lead to high efforts tuning the weighting factors of the objective function G.

The tracking error for each output variable y_i is quantified as follows

$$g_{y_i}\left(\underline{y}\left(\underline{p}\right)\right) = \int_{t_0}^{t_e}\left(\frac{y_i\left(t,\underline{p}\right) - y_{i,cmd}(t)}{y_{i,max}}\right)^2 dt. \tag{22}$$

Thus, the tracking error of the different output variables is normalized to the maximum range $y_{i,max}$, squared and integrated over the simulation time. The overall tracking error is then calculated as the sum of all single tracking errors, as follows:

$$g_y\left(\underline{y}\left(\underline{p}\right)\right) = \sum_{i=1}^{q} g_{y_i}\left(\underline{y}\left(\underline{p}\right)\right). \tag{23}$$

The state-dependent cost functional g_x quantifies additional design objectives which are not incorporated in the cost functional dependent on the output variable tracking. In case of the tiltrotor VTOL, this is the torsion torque around the body-fixed ${}_fy$-axis of

the aircraft resulting from the propellers. This characteristic must be included in the cost functional due to the following reason: An efficient way to produce yawing torque for the presented VTOL is to use the propeller's drag torque. However, this creates a considerable torsional torque around the ${}_f y$-axis. This results in high structural torques that cause considerable deformations in the main wing. In combination with the remaining noise of the sensor measurements, as well as the mass of the propellers and tilting mechanisms and their large distances from the ${}_f y$-axis, this can lead to structural oscillations which must be avoided. The presented VTOL can also create a yawing torque utilizing the tilt angles, which results in no additional torsional torque around the ${}_f y$-axis of the aircraft and is hence desirable. Since the model presented in Section 5.1 considers the aircraft as a rigid body, this must be included in the cost functional g_x as follows:

$$g_x\left(\underline{x}\left(\underline{p}\right)\right) = \int_{t_0}^{t_e} \left(M_T\left(\underline{x}\left(t, \underline{p}\right)\right)\right)^2 dt. \tag{24}$$

The integral of the squared torsional torque of the propellers around the ${}_f y$-axis of the aircraft over the simulation time is included in g_x. This is required in order to find parameters $\underline{p}$ that use the actuators in a way that ensures the torsional torque acting on the mechanical structure of the aircraft is minimized.

5.3. Reference Trajectory/Mission

To receive parameter sets which can be utilized for the tiltrotor VTOL, all relevant state areas have to be covered within the simulation. Fulfilling this requirement, the reference trajectory must be chosen so that it includes the typical operating range of the aircraft. The operating range of the tiltrotor VTOL mainly consists of hover, transition, and airborne flight. In all these state areas, the aircraft must be able to stabilize itself and also provide good tracking of the commanded output variables. Typical test trajectories quantifying the controller quality are step responses. However, due to the nonlinear characteristics of the aircraft, the direction of a step has an impact on the dynamic behavior. Doublets which are symmetric references ensure that a step in both directions is conducted. Hence, all relevant dynamic characteristics are included. Since the attitude control is addressed, these doublets are commanded for roll angle, pitch angle, and yaw rate, characterizing the controller quality.

In order to test controller quality, these doublets are commanded for hover, transition, and airborne flight. The different state areas are mainly quantified by the aircraft's overall tilt angle as well as the aerodynamic speed. Since the tilt angle in particular adds complexity in terms of nonlinearity, the state area is defined using the overall tilt angle. It is obvious that the hover mode is characterized by an overall tilt angle of $\delta = 0$ and the airborne mode by a tilt angle of $\delta = \pi/2$. The transition between these two modes mainly covers everything in between. In order to ensure a reasonable simulation time for an objective function evaluation and to also avoid prioritizing the transition mode over hover and airborne flight, just one additional sample point at $\delta = \pi/4$ is considered. This includes the especially complex nonlinear characteristics during the transition but at the same time adds only one sample point during transition. Although only rotational degrees of freedom are considered, the commanded overall thrust as well as the aerodynamic velocity are selected so that the aircraft's drag and the gravitational force are approximately compensated, making sure the simulation covers the relevant state areas. The reference trajectory is shown in Figure 7.

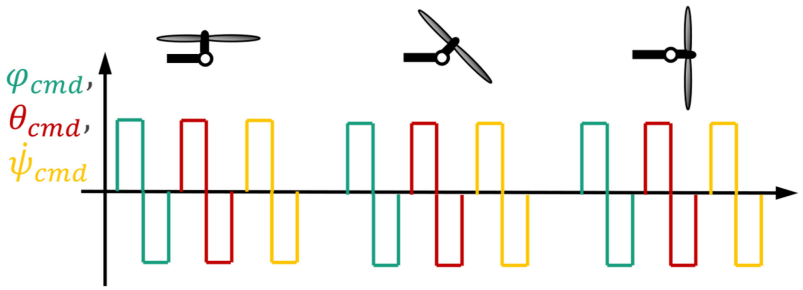

Figure 7. Reference trajectory for objective function evaluation.

5.4. Optimization Algorithm

The optimization algorithm must be chosen based on the characteristics of the optimization problem. Since the calculation of the objective function is conducted using a numerical solver within a simulation environment it is not available in analytical form. Thus, calculation of a gradient is not analytically possible. Additionally, the simulation is computationally costly. Thus, calculation of the objective function is time consuming as well. Furthermore, no reasonable initial value guess is available.

Different optimization algorithms can be considered on this basis. Metaheuristics are suitable and performant approaches solving optimization problems within a reasonable amount of time. Although these algorithms often do not find the global optimum, they are suitable approaches for finding a good solution in cases where little information is available about the objective function. Well-known algorithms are, for example, simulated annealing, ant colony optimization, particle swarm optimization as well as genetic algorithms [28,29]. Another method capable of solving such black box optimization problems with computationally expensive cost functionals is surrogate optimization [30]. In order to select a suitable algorithm, the performances of genetic algorithms, particle swarm optimization, and surrogate optimization are tested based on the optimization problem presented within this paper. Particle swarm optimization and genetic algorithms are promising approaches, since these are population-based solvers and therefore explore a large area of the solution space. This is especially beneficial since no initial value is available. However, since they are population-based approaches a rather large number of objective function evaluations per iteration is necessary. Therefore, surrogate optimization is also considered as a potential optimization algorithm because it approximates the objective function and consequently reduces objective function calculations and computing efforts. Surrogate optimization also does not require an initial guess. A practical reason for selecting these algorithms is their availability within commercial software. This is especially important because the aim of the automated parameter tuning approach is to reduce effort.

The optimization results are shown in Figure 8. The considered algorithms perform different amounts of objective function evaluations per iteration. Hence, making the results comparable, the best objective function values are plotted over the amount of objective function evaluations. Particle swarm optimization delivers the best results. However, it only performs slightly better than surrogate optimization. Additionally, the particle swarm optimization provides a more continuous improvement in the objective function value. The genetic algorithm performs worse than the other algorithms. Since particle swarm optimization delivers the best results, it is utilized for all further optimizations. However, surrogate optimization is also a feasible option, since the best objective function value is less than 1% worse than the best objective function value identified by particle swarm optimization.

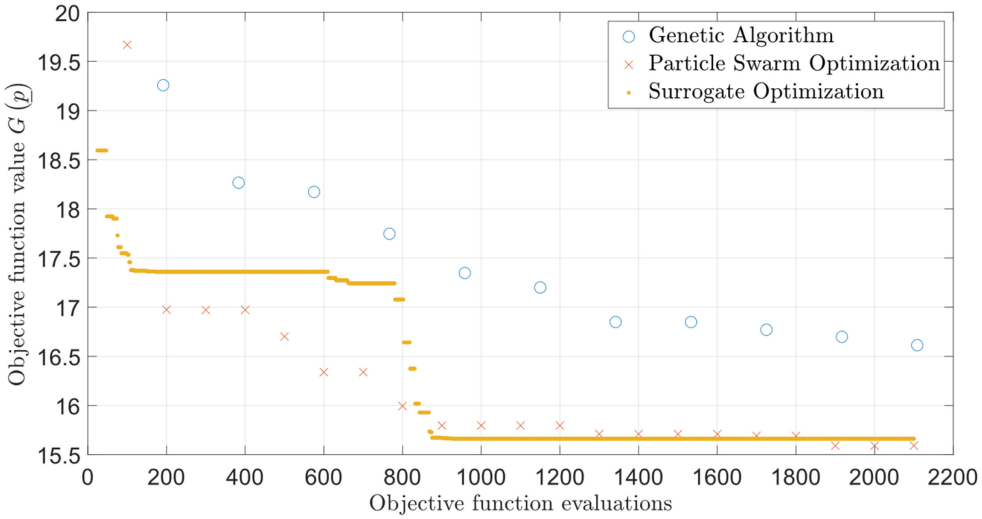

Figure 8. Performance of optimization algorithms for automated parameter tuning approach.

6. Results

This section presents the optimization results validating the automated parameter tuning approach. Therefore, model-based validation of the identified parameters is conducted first. This shows that it is possible to find a sufficient parameter set within the modeling environment. Afterwards, real-world validation of the identified parameters is conducted. For that purpose, a 4-DOF testbench is presented, enabling risk-minimized validation of the presented approach. On this basis, different pareto-optimal parameter sets are identified specifically for the testbench scenario considering output variable tracking as well as torsional torque. Finally, a suitable parameter set is tested and validated conducting experiments using the real aircraft on the testbench.

The model-based result of the parameter tuning is shown in Figure 9. Since the attitude control loop parameters are tuned, only rotational degrees of freedom are considered. The overall tilt angle is determined by the reference trajectory in order to cover hover, transition, and airborne flight. Hence, specific thrust and aerodynamic velocity were selected making sure the aircraft is in a realistic steady state. The doublets for yaw rate were reduced in length and size in states with aerodynamic velocity, ensuring the slip angle remains within realistic limits. Figure 9 shows that it is possible to automatically tune control allocation parameters since all state variables show sufficient tracking and good decoupling. Couplings can only be seen in some rare cases, and these are always compensated quickly. It can also be seen that controller speed decreases in airborne flight. A possible reason for this is aerodynamic damping, since it is a known problem of INDI already investigated in [11]. It can be tackled using a feedforward control. Another possible reason are the slower actuator dynamics of the control surfaces. In addition, it can be seen that in state areas with aerodynamic velocity the stationary accuracy of the yaw rate decreases. This can also be caused by the aerodynamic damping. Furthermore, sensor noise is not affecting the aircraft dynamics significantly. Summing up, it is possible to automatically identify a parameter set resulting in a stable and sufficient controller quality within the simulation environment. Thus, a significant amount of parameter tuning efforts can be saved.

Hence, the automated parameter tuning approach shows functional results within a model-based environment. Therefore, the next step consists of real-world testing and validation of the identified parameter set. However, testing the identified parameter set in free flight poses a certain risk for a crash. Therefore, a safe and realistic testing environment is required. A possible testing environment for drones is a 4-degrees-of-freedom testbench. Such testbenches enable movements along the rotational degrees of freedom as well as the vertical translational degree of freedom within certain boundaries. The horizontal translational degrees of freedom are blocked. Thus, it is possible to test the

attitude stabilization in hover mode using the testbench. Since unusual movements beyond the typical operating range are blocked by a mechanical stop the attitude control and stabilization can be tested at minimal risk. This is especially beneficial since the rotational dynamics are of utmost importance for the aircraft's stability. Additionally, in the case of the presented aircraft configuration, it is possible to test the performance of the INDI controller approach in highly nonlinear state areas. A possible scenario would be to tilt the propellers forward resulting in a nonlinear state area. Therefore, this testbench is well suited for testing the performance of the INDI approach and thus also the automatically tuned parameters. The testbench is shown in Figure 10, consisting of a cardan joint where the aircraft is attached very close to the aircraft's center of mass. Additionally, a translational joint allows for vertical translational movement.

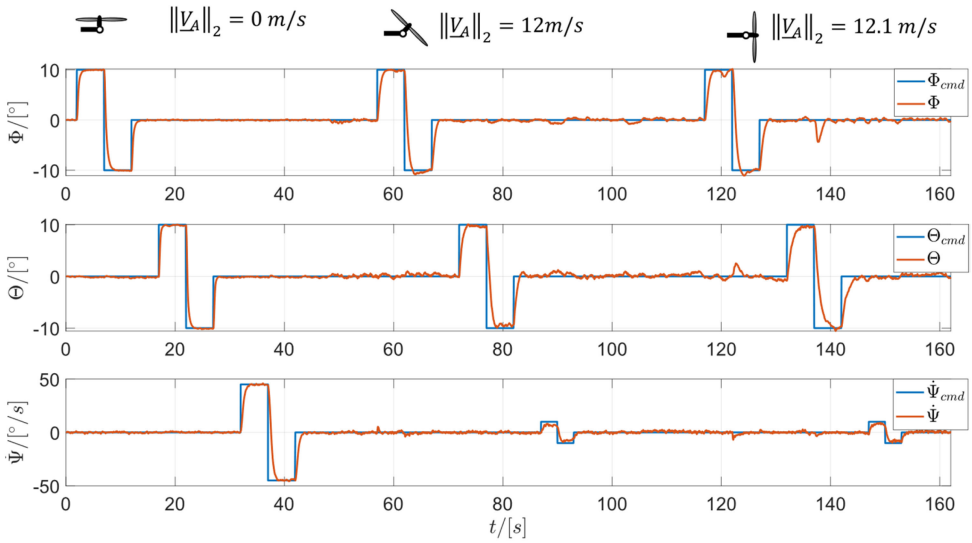

Figure 9. Model-based results of automatically tuned parameters.

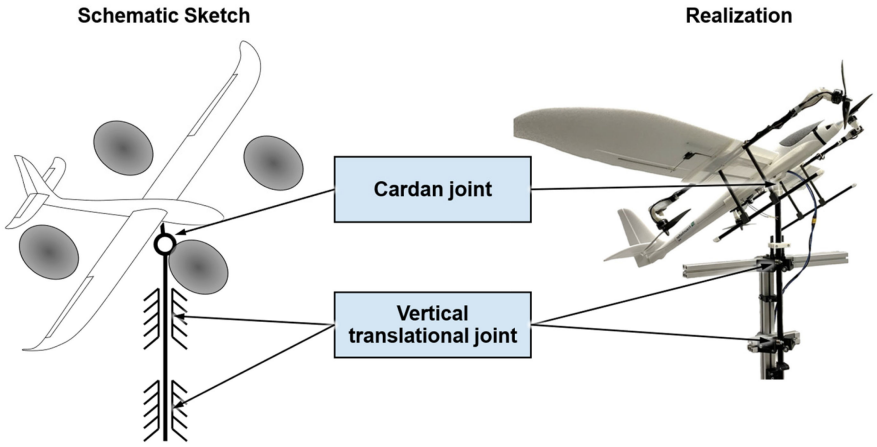

Figure 10. Illustration showing 4-degrees-of-freedom testbench.

Using this 4-DOF testbench seems to be a reasonable step validating the automated parameter tuning approach. Since the testbench only reflects reality within certain limits some assumptions must be made. The testbench is fixed to the earth and not included within a wind tunnel. Therefore, state areas with aerodynamic velocities cannot be tested. Hence, the aerodynamic control surfaces have no control effectiveness regarding the pseudo controls. Consequently, the already-presented parameter set which included aerodynamic speed is not sufficient for testing the aircraft on the testbench. For the sake of validating the automated parameter tuning approach at a minimum risk, new parameters have to be

tuned, neglecting aerodynamics. The reference trajectory itself remains the same in order to include system complexity especially resulting from the nonlinear tilting process. In order to obtain a parameter set which is functional in reality, different pareto-optimal solutions have been identified. This is performed varying γ, which weights the conflict of minimum output variable tracking error, and minimum torsional torque induced into the mechanical structure of the aircraft. In this context, pareto-optimality of a solution means that it is not possible to improve output variable tracking without deteriorating torsional torque and vice versa. The identified pareto-optimal solutions are depicted in Figure 11. Considering the objective functions described in Section 5.2, an interpretation of the absolute objective function values is difficult. But in relation to each other, it can be seen that a reduction in g_x by more than 50% is possible while g_y increases by less than 10%. Hence, a significant reduction in torsional torque only results in a minor reduction in output variable tracking.

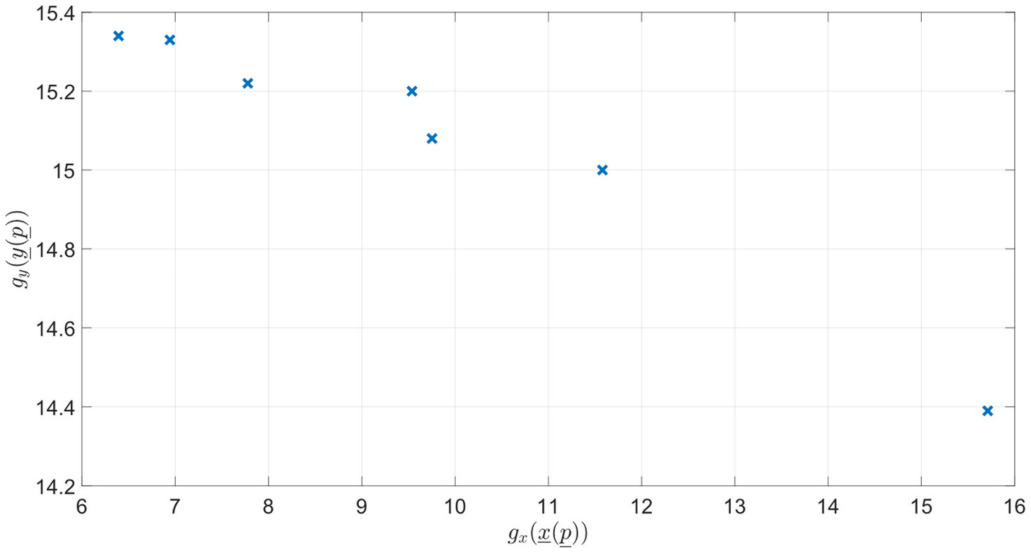

Figure 11. Pareto-optimal solutions of testbench specific optimization.

These pareto-optimal parameter sets are tested on the testbench. Based on these tests, a parameter set not resulting in torsional oscillations and providing good output variable tracking was selected for further analysis. To evaluate the performance of automatically tuned parameter sets, they are compared to a manually identified parameter set. The results of testbench experiments using the automatically tuned parameter set and the manually tuned parameter set are shown in Figure 12. Both parameter sets show good stability and reference trajectory tracking. The decoupling characteristics are sufficient even in highly nonlinear state areas. In state areas with an overall tilt angle close to 90° the aircraft shows slight oscillations. This is basically due to the testbench: The control effectiveness of the propellers and tilt angles decreases with regard to the roll and pitch axis, and because of lacking aerodynamic speed, the control surfaces do not provide any control effectiveness. However, this shows the high performance of the controller approach. Comparing both results, it can be concluded that the automatically tuned control allocation parameters result in an even better control quality since the aircraft shows less oscillations, less overshooting and the same speed in all degrees of freedom. Thus, automated parameter tuning for the control allocation of an INDI-based controller is possible and reduces manual tuning efforts. Hence, the presented approach is validated.

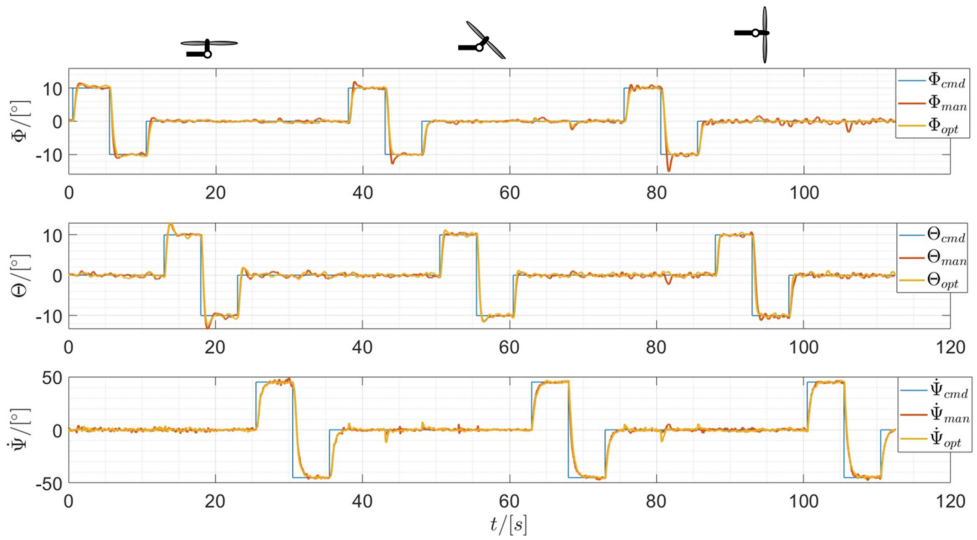

Figure 12. Trajectory tracking comparison of automatically and manually tuned parameters.

7. Conclusions and Outlook

This paper presented and investigated an automated tuning approach for the parameters of an INDI-based control allocation. For that purpose, a tiltrotor VTOL aircraft as well as an INDI-based controller for that aircraft were introduced. In terms of the INDI approach, control allocation parameters, which have to be tuned, were presented. On that basis, the automated parameter tuning approach was presented, consisting of a simulation environment, a reference trajectory, an objective function, and an optimization algorithm. The simulation environment incorporates a model of the tiltrotor VTOL. This rigid body model considers simplified actuator dynamics, a propeller model, a component-based aerodynamics model, and a sensor noise model. This simulation environment is used to calculate the objective function quantifying the design target. This specifically consists of the output variable tracking error as well as the torsional torque acting on the aircraft. The first target considers the controller quality and the second target preserves structural integrity avoiding torsional oscillations around the aircraft's lateral axis. The reference trajectory consists of doublets in hover, transition, and airborne mode for all relevant output variables. This ensures maneuverability within all relevant state areas of the aircraft. The particle swarm algorithm was selected as the optimization algorithm. Based on the parameter tuning approach control allocation parameters of the attitude control loop were identified successfully. These parameters were identified in general and also specifically for the aircraft on the 4-DOF testbench. Using the testbench, the identified parameters were successfully validated on the real system. The automatically tuned parameters show even better performance than manually tuned parameters. Summing up, this paper has successfully shown the feasibility of an automated parameter tuning approach for the control allocation of an INDI-based controller using the example of a tiltrotor VTOL. It has therefore shown the potential of the presented approach for reducing manual tuning efforts.

Future work lies in the real-world validation of tuned parameters in state areas with aerodynamic speed. Furthermore, the parameters of the velocity control loop have to be identified using the presented approach. In addition, the focus of this paper was to show the general feasibility of automated parameter tuning for the control allocation. Therefore, only a limited number of suitable optimization algorithms were tested regarding their performance. However, a large variety of other suitable and performant optimization algorithms exist. Hence, future work consists of testing their performance automatically tuning parameters of the control allocation. Finally, this approach can be validated using another aircraft configuration or another INDI structure. Finally, the presented controller structure can be extended using a reference model.

Author Contributions: Conceptualization, M.H.; methodology, M.H.; software, M.H. and F.S.; validation, M.H., U.N. and F.S.; formal analysis, M.H.; investigation, M.H.; resources, M.H. and U.N.; writing—original draft preparation, M.H.; writing—review and editing, F.S.; visualization, M.H. and F.S.; supervision, C.H. and A.T.; project administration, C.H. and U.N. All authors have read and agreed to the published version of the manuscript.

Funding: This research received no external funding.

Data Availability Statement: Data are contained within the article.

Acknowledgments: The authors thank Stephan Myschik for revising and reviewing the manuscript.

Conflicts of Interest: The authors declare no conflicts of interest.

References

1. Akkinapalli, V.S.; Holzapfel, F. Incremental Dynamic Inversion based Velocity Tracking Controller for a Multicopter System. In Proceedings of the 2018 AIAA Guidance, Navigation, and Control Conference, Kissimmee, FL, USA, 8–12 January 2018.
2. Smeur, E.; de Croon, G.; Chu, Q. Cascaded incremental nonlinear dynamic inversion for MAV disturbance rejection. *Control Eng. Pract.* **2018**, *73*, 79–90. [CrossRef]
3. Smeur, E.J.J.; Chu, Q.; de Croon, G.C.H.E. Adaptive Incremental Nonlinear Dynamic Inversion for Attitude Control of Micro Air Vehicles. *J. Guid. Control Dyn.* **2016**, *39*, 450–461. [CrossRef]
4. Sieberling, S.; Chu, Q.P.; Mulder, J.A. Robust Flight Control Using Incremental Nonlinear Dynamic Inversion and Angular Acceleration Prediction. *J. Guid. Control Dyn.* **2010**, *33*, 1732–1742. [CrossRef]
5. Grondman, F.; Looye, G.; Kuchar, R.O.; Chu, Q.P.; Van Kampen, E.-J. Design and Flight Testing of Incremental Nonlinear Dynamic Inversion-based Control Laws for a Passenger Aircraft. In Proceedings of the 2018 AIAA Guidance, Navigation, and Control Conference, Kissimmee, FL, USA, 8–12 January 2018.
6. Raab, S.A.; Zhang, J.; Bhardwaj, P.; Holzapfel, F. Proposal of a Unified Control Strategy for Vertical Take-off and Landing Transition Aircraft Configurations. In Proceedings of the 2018 Applied Aerodynamics Conference, Atlanta, GA, USA, 25–29 June 2018.
7. Hein, L.; Panchal, P.; Surmann, D.; Myschik, S. Performance Analysis of an electrically powered General Aviation Aircraft using parallelized automated Mission Simulations. In Proceedings of the AIAA AVIATION 2023 Forum, San Diego, CA, USA & Online, 12–16 June 2023.
8. Di Francesco, G.; D'Amato, E.; Mattei, M. INDI Control with Direct Lift for a Tilt Rotor UAV. *IFAC-PapersOnLine* **2015**, *48*, 156–161. [CrossRef]
9. Di Francesco, G.; Mattei, M. Modeling and Incremental Nonlinear Dynamic Inversion Control of a Novel Unmanned Tiltrotor. *J. Aircr.* **2016**, *53*, 73–86. [CrossRef]
10. Di Francesco, G.; Mattei, M.; D'Amato, E. Incremental Nonlinear Dynamic Inversion and Control Allocation for a Tilt Rotor UAV. In Proceedings of the AIAA Guidance, Navigation, and Control Conference, National Harbor, MD, USA, 13–17 January 2014.
11. Binz, F. Robust, Fault-Tolerant Control of Aircraft with Hovering Capability. Ph.D. Thesis, Rheinisch-Westfälische Technische Hochschule Aachen, Aachen, Germany, 2020. [CrossRef]
12. Binz, F.; Islam, T.; Moormann, D. Attitude control of tiltwing aircraft using a wing-fixed coordinate system and incremental nonlinear dynamic inversion. *Int. J. Micro Air Veh.* **2019**, *11*, 1756829319861370. [CrossRef]
13. Milz, D.; Looye, G. Tilt-Wing Control Design for a Unified Control Concept. In Proceedings of the AIAA SCITECH 2022 Forum, San Diego, CA, USA, 3–7 January 2022.
14. Lovell-Prescod, G.H.; Ma, Z.; Smeur, E.J. Attitude Control of a Tilt-rotor Tailsitter Micro Air Vehicle Using Incremental Control. In Proceedings of the 2023 International Conference on Unmanned Aircraft Systems (ICUAS), Warsaw, Poland, 6–9 June 2023; pp. 842–849.
15. Pfeifle, O.; Fichter, W. Energy Optimal Control Allocation for INDI Controlled Transition Aircraft. In Proceedings of the AIAA Scitech 2021 Forum, Online, 11–15 January 2021.
16. Lombaerts, T.; Kaneshige, J.; Schuet, S.; Aponso, B.L.; Shish, K.H.; Hardy, G. Dynamic Inversion based Full Envelope Flight Control for an eVTOL Vehicle using a Unified Framework. In Proceedings of the AIAA Scitech 2020 Forum, Orlando, FL, USA, 6–10 January 2020.
17. de Ponti, T.; Smeur, E.; Remes, B. Incremental Nonlinear Dynamic Inversion controller for a Variable Skew Quad Plane. In Proceedings of the 2023 International Conference on Unmanned Aircraft Systems (ICUAS), Warsaw, Poland, 6–9 June 2023; pp. 241–248.
18. Karssies, H.J.; de Wagter, C. Extended incremental non-linear control allocation (XINCA) for quadplanes. *Int. J. Micro Air Veh.* **2022**, *14*, 17568293211070825. [CrossRef]
19. Zhang, J.; Bhardwaj, P.; Raab, S.A.; Saboo, S.; Holzapfel, F. Control Allocation Framework for a Tilt-rotor Vertical Take-off and Landing Transition Aircraft Configuration. In Proceedings of the 2018 Applied Aerodynamics Conference, Atlanta, GA, USA, 25–29 June 2018.

20. Bhardwaj, P.; Raab, S.A.; Zhang, J.; Holzapfel, F. Integrated Reference Model for a Tilt-rotor Vertical Take-off and Landing Transition UAV. In Proceedings of the 2018 Applied Aerodynamics Conference, Atlanta, GA, USA, 25–29 June 2018.
21. Slotine, J.; Li, W. *Applied Nonlinear Control*, 1st ed.; Prentice-Hall International: Englewood Cliffs, NJ, USA, 1991.
22. Henkenjohann, M.; Nolte, U.; Henke, C.; Trächtler, A. Novel Cascaded Incremental Nonlinear Dynamic Inversion Controller Approach for a Tiltrotor VTOL. In Proceedings of the 2023 International Conference on Unmanned Aircraft Systems (ICUAS), Warsaw, Poland, 6–9 June 2023; pp. 1097–1105.
23. van 't Veld, R.; van Kampen, E.-J.; Chu, Q.P. Stability and Robustness Analysis and Improvements for Incremental Nonlinear Dynamic Inversion Control. In Proceedings of the 2018 AIAA Guidance, Navigation, and Control Conference, Kissimmee, FL, USA, 8–12 January 2018.
24. Steffensen, R.; Steinert, A.; Mbikayi, Z.; Raab, S.; Angelov, J.; Holzapfel, F. Filter and sensor delay synchronization in incremental flight control laws. *Aerosp. Syst.* **2023**, *6*, 285–304. [CrossRef]
25. Hartmann, P. *Vorausschauende Flugbahnregelung für Kippflügelflugzeuge: Predictive Flight Path Control for Tilt-Wing Aircraft*; Rheinisch-Westfälische Technische Hochschule Aachen: Aachen, Germany, 2017.
26. Schütt, M.; Tobias, I.; Philipp, H.; Moormann, D. Scalable Design Approach to Analyze Flight Mechanical Performance of Tilt-Wing UAVs. In Proceedings of the 31st Congress of the International Council of the Aeronautical Sciences, Belo Horizonte, Brazil, 9–14 September 2018.
27. May, M.S.; Milz, D.; Looye, G. Semi-Empirical Aerodynamic Modeling Approach for Tandem Tilt-Wing eVTOL Control Design Applications. In Proceedings of the AIAA SCITECH 2023 Forum, National Harbor, MD, USA & Online, 23–27 January 2023.
28. Tsai, C.-W.; Chiang, M.-C. *Handbook of Metaheuristic Algorithms: From Fundamental Theories to Advanced Applications*; Elsevier: Amsterdam, The Netherlands, 2023.
29. Cuevas, E.; Diaz, P.; Camarena, O. *Metaheuristic Computation: A Performance Perspective*; Springer International Publishing: Cham, Switzerland, 2021.
30. Gutmann, H.-M. A Radial Basis Function Method for Global Optimization. *J. Glob. Optim.* **2001**, *19*, 201–227. [CrossRef]